International Scientific Conference

SURFACTANTS AND DISPERSED SYSTEM IN THEORY AND PRACTICE

PROCEEDINGS

SCIENTIFIC EDITOR
KAZIMIERA ANNA WILK

SURFAKTAKNTY I UKŁADY ZDYSPERGOWANE W TEORII I PRAKTYCE

Politechnika Wrocławska

SURUZ SCIENTIC NETWORK

Politechnika
Wrocławska

International Scientific Conference

SURFACTANTS AND DISPERSED SYSTEMS IN THEORY AND PRACTICE

W TEORII I PRAKTYCE

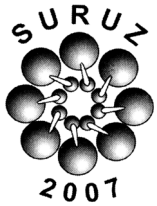

Książ Castle
May 22-24, 2007

SURFAKTAKNTY I UKŁADY ZDYSPERGOWANE

Organized by Faculty of Chemistry, Wrocław University of Technology

In cooperation with

- Scientific Network SURUZ *SURFACTANTS AND DISPERSED SYSTEMS IN THEORY AND PRACTICE* (contract No. INCO-CT-2003-003355)

Under auspices of

- Polish Chemical Society, Wrocław
- Polish Association of Chemical Engineers, Wrocław
- Dean of Faculty of Chemistry, Wrocław University of Technology, Wrocław

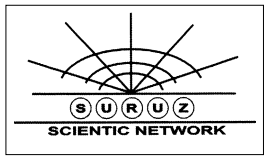

SCIENTIFIC EDITOR
KAZIMIERA ANNA WILK

PALMApress
53-413 Wrocław, pl. Hirszfelda 16/17
tel. 071 338 14 11, 071 338 14 12
www.palmapress.pl

ISBN 83-7076-125-9

Pavol BALGAVÝ[*], Ferdinand DEVÍNSKY[**], Jana GALLOVÁ[*],
Janka KARLOVSKÁ[*], Norbert KUČERKA[*], Ivan LACKO[**], Daniela UHRÍKOVÁ[*]

EFFECTS OF SURFACTANTS ON THE STRUCTURE OF MODEL MEMBRANES

Effects of biocidal surfactants *N*-alkyl-*N*,*N*-dimethylamine-*N*-oxides (*CnNO*, *n*=8-18 is the even number of carbons in alkyl substituent) on fluid model bilayers prepared from synthetic dioleoylphosphatidylcholine (*DOPC*), dipalmitoyphosphatidylcholine (*DPPC*), natural egg yolk phosphatidylcholine (*EYPC*) were studied using spin label ESR spectroscopy, small-angle neutron scattering, x-ray diffraction, turbidimetry, ^{31}P NMR spectroscopy and differential scanning calorimetry. *CnNO* molecules partition into the bilayer between phospholipids and create structural defects in its hydrophobic region and change the lipid conformation in its polar region. Depending on the *CnNO* partition coefficients and alkyl and lipid acyl chain lengths mismatch, phase transitions, bilayer thickness and surface area and the probability of *gauche* conformer formation in hydrocarbon chains are modulated at lower *CnNO*:lipid molar ratios; at higher ratios, the bilayer is destabilized and mixed *CnNO*-phospholipid micelles are formed. Selected results of these studies are reviewed and correlated with the *CnNO* biocidal effects and with their effect on the activity of sarcoplasmic reticulum Ca^{2+}-ATPase (SERCA) reconstituted into *DOPC* bilayers.

1. INTRODUCTION

N-Alkyl-*N*,*N*-dimethylamine-*N*-oxides (*CnNO*, *n* is the number of carbon atoms in the alkyl substituent) with a strong polar N-O bond and a high electron density on the oxygen are zwitterionic surfactants at physiological values of pH [1]. They are widely used in pharmaceutical and cosmetic formulations and as detergents in household dishwashing liquids and surface cleaners. *CnNO* surfactans, in particular *C10NO* and *C12NO*, are also used for the isolation, purification, reconstitution and crystallization of membrane proteins [2]. *CnNO*s display microbicidal [3], phytotoxic [4], immunomodulatory [5], algicidal and antiphotosynthetic [6, 7] activities. We have also found that *CnNO*s inhibit the phosphohydrolase activity of the transmembrane Ca^{2+}-transporting sarcoplasmic reticulum ATPase (SERCA) [8].

The dependencies of biological potencies on the *CnNO* alkyl chain length *n* display a typical "cut-off" course - the ability to affect the biological function progressively increases with the increase of *n* up to a maximum and than decreases (see selected examples in Fig. 1). This deviation from the Meyer-Overton rule [9,10] is a general phenomenon and it has been observed in various biological activities in practically every amphiphile homologous series as a function of the length of linear hydrocarbon substituent [11]. It is

[*] Department of Physical Chemistry of Drugs, Faculty of Pharmacy, Comenius University, Odbojárov 10, 832 32 Bratislava, Slovak Republic
[**] Department of Chemical Theory of Drugs, Faculty of Pharmacy, Comenius University, Odbojárov 10, 832 32 Bratislava, Slovak Republic

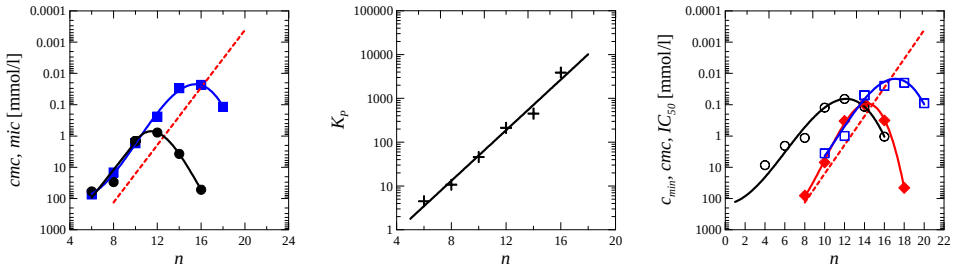

Fig. 1. Dependence of the critical micelle concentration cmc (dashed line), of the partition coefficient K_P between the water and bilayers from *Escherichia coli* isolated phospholipids (full line), of the *Escherichia coli* (●) and *Staphylococcus aureus* (■) minimum inhibition concentration *mic*, of the half maximum inhibition concentration IC_{50} and of *Vicia sativa L.* seedling root growth (○) and of Hill reaction in chloroplasts (♦), and of the sarcoplasmic reticulum ATPase minimum inhibition concentration c_{min} (□), on the *CnNO* alkyl chain length *n*. The *cmc*, K_P and *mic* values were taken from [3], the IC_{50} values from [4, 7], and the c_{min} values from [8].

noteworthy that the decrease occurs when the effective concentration of long-chain homologues reaches the critical micelle concentration *cmc*. The simplest explanation of the "cut-off"-type curves in Fig. 1 could therefore be the change of *CnNO* partition equilibrium of *CnNO* monomers between the site of action and the aqueous solution for short-chain homologues to a more complicated partition equilibrium of *CnNO* between the site of action, aqueous solution and micelles for long-chain *CnNO* homologues. Because of the amphiphilic character of *CnNO* surfactants, their primary site of action is the phospholipid bilayer, the structural matrix of biological membranes. We have observed that the partition coefficient K_P between the aqueous phase and lipid bilayers prepared from bacterial phospholipids increases exponentially with the *CnNO* alkyl chain length without any indications of anomalies at chain lengths *n*=12-16 where the the cut-off effects are observed (see Fig. 1).

The partition equilibria certainly play an important role in the biological activities of surfactants. Minimally equally important are, however, mutual interactions of surfactants with biomembrane constituents. In our contribution, examples of *CnNO* effects on selected physical properties of lipid bilayers are shortly reviewed.

2. RESULTS

In the phospholipid bilayer, the polar fragment of *CnNO* interacts with polar fragments of phospholipids and the *CnNO* alkyl chain with the phospholipid hydrocarbon chains. The insertion of *CnNO* molecules between phospholipids results in the lateral bilayer expansion. Due to the hydrophobic mismatch, *CnNO* with alkyl chain shorter than phospholipid chains creates voids in the bilayer hydrophobic region, and this is compensated by a *trans-gauche* isomerisation of hydrocarbon chains or by their interdigitation. We have studied these effects using stearic acid spin probes, labeled with the paramagnetic dimethyloxazolidinyl group on the m-th carbon (*m-DSA*, *m*=13, 16), located in the fluid hydrated bilayers of egg yolk phosphatidylcholine (*EYPC*). The averaged length of the *EYPC* acyl chain is 17.8 carbons with 1.2 double bonds [12] and the *EYPC* bilayers are fluid above 0°C, even at low hydration used to avoid partitioning between bilayers and the aqueous phase. The order parameters *S* obtained from the ESR spectra are frequently used

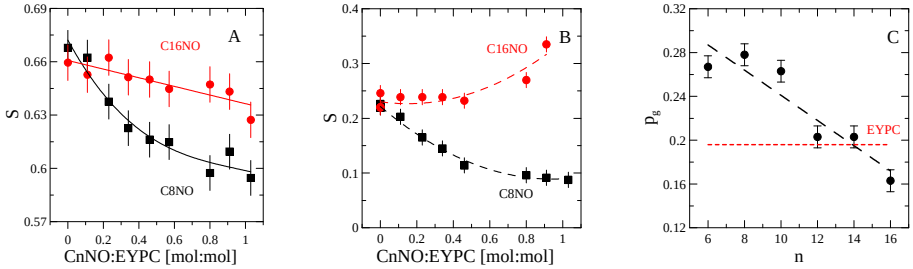

Fig. 2. Order parameter *S* of *13-DSA* (panel A) and *16-DSA* (B) spin probes as a function of *CnNO*:*EYPC* molar ratio and probability of gauche conformers formation p_g as a function of *CnNO* chain length *n* (C) at *CnNO*:*EYPC*=0.8 molar ratio. The horizontal dashed line shows the p_g value at *CnNO*:*EYPC*=0 molar ratio. The data were obtained at 5ºC. The samples were hydrated from the gaseous phase over saturated NaCl solution in H_2O.

as measures of bilayer fluidity; their dependencies in Figs. 2A and B indicate that *CnNO*s affect the bilayer hydrophobic structure depending on the concentration in the bilayer and alkyl length. From the known values of order parameters determined with two different spin labels, the probability of *gauche* conformations p_g can be obtained [13]. The results in Fig. 2C prove the predicted effect – the disordering of the bilayer hydrocarbon region by *CnNO*s decreases with their alkyl length *n*; the ordering induced by *C16NO* indicates a chain interdigitation

Other effects of insertion of *CnNO*s into bilayer are a modulation of bilayer thickness at lower bilayer concentrations and a bilayer destabilization at higher concentrations. A suitable method to study these effects is the small-angle neutron scattering (SANS). From the SANS spectra of lipid aggregates in D_2O, two parameters can be easily evaluated [14, 15]: The shape parameter *r*=1 is observed in unilamellar vesicles (ULV) and bilayer sheets, *r*=2 in cylindrical micelles and *r*=3 in globular micelles; for *r*=1, the scattering density weighted bilayer thickness d_g is obtained. We have prepared dioleoylphosphatidylcholine (*DOPC*) and *CnNO* mixtures at various *CnNO*:*DOPC* molar ratios in D_2O and extruded them through 50 nm filters. The extrusion produces ULVs from aqueous dispersions of multilamellar vesicles (MLV) from *DOPC* [16]. Using SANS, we have confirmed that increasing of *CnNO*:*DOPC* ratio **in sample,** the bilayer becomes destabilized and micelles form in dispersions; *C18NO* is less potent in this destabilization than *C12NO* (Fig. 3), though the *CnNO*:*DOPC* molar ratio **in bilayer** is

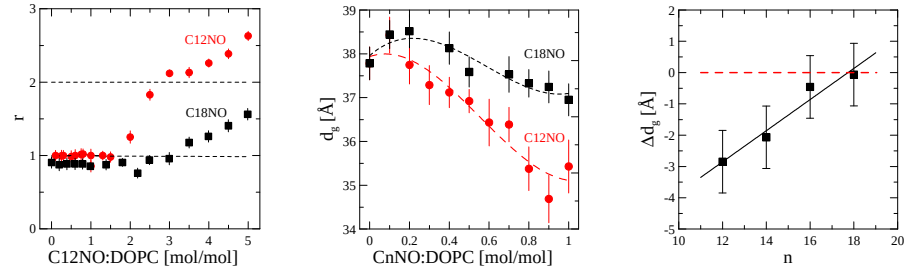

Fig. 3. Shape parameter *r* and bilayer thickness d_g as a function of *CnNO*:*DOPC* molar ratio in the sample for *n*=12 (●) and *n*=18 (■), and the change of bilayer thickness Δd_g as a function of *CnNO* alkyl length *n* at *CnNO*:*DOPC*=1 molar ratio in the sample. The *DOPC* concentration in the sample was 10 mg/ml.

higher for *C18NO* due to its higher K_P (Fig. 1). For samples with r=1, the bilayer thickness d_g was calculated. The data in Fig. 3 clearly demonstrate that *CnNO*s influence the bilayer stability and thickness; the effects are more pronounced for shorter *CnNO* homologues. At higher *CnNO*:*DOPC* molar ratios (1:1), the thickness change as a function of *CnNO* alkyl length n evidently correlates with the p_g change (Fig. 2C). We have observed the same trend of thickness change in partially hydrated fluid bilayers in a lamellar phase of *EYPC* using small-angle X-ray diffraction [25].

The bilayer – micelle transition, also termed solubilization, can be conviently studied by turbidimetry. Using this method, we confirmed that the capability of *CnNO*s to solubilize ULVs [17] and MLVs [18] from *EYPC* in excess of water continuously decreases with the increase of alkyl chain length n. In case of 100 nm extruded ULVs from *DOPC* and *C12NO*, we studied the solubilization in more detail (Fig. 5). During step-wise additions of *C12NO* aliquots to ULV dispersion, the turbidity changes in 3 stages (Fig. 5A) in agreement with the phase behaviour of bilayer-forming lipid –

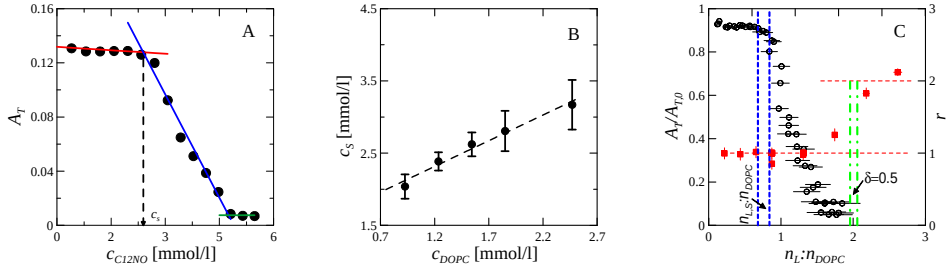

Fig. 5. Turbidity A_T of *DOPC* (1.235 mM) unilamellar vesicles as a function of c_{C12NO} concentration (A), dependence of the solubilization concentration c_S on the *DOPC* concentration c_{DOPC} (B), and dependencies of normalized turbidity $A_T/A_{T,0}$ and SANS shape parameter r on the *C12NO*:*DOPC* molar ratio in bilayer, $n_L:n_{DOPC}$. The *C12NO*:*DOPC* molar ratio in bilayer at the onset of solubilization, $n_{LS}:n_{DOPC}$, and at the bilayer – nonbilayer micelle transition (predicted by packing parameter δ) is delimited by dashed and dash-dotted vertical lines, respectively.

micelle-forming surfactant mixed systems in an excess of water (reviewed in [19]): in the stage I, the liposomes with surfactant intercalated into lipid bilayers (mixed bilayers) are in equilibrium with free surfactant molecules in the aqueous phase; in the stage II, the mixed bilayers coexist with mixed lipid – surfactant micelles and free surfactant molecules in the aqueous phase; in the stage III, the mixed lipid – surfactant micelles are in equilibrium with free surfactant molecules in the aqueous phase. From the simultaneous fitting of the data by linear functions, the solubilizing concentration of surfactant c_S is obtained as the onset concentration corresponding to the intersection of lines approximating the data in the stage I and II. We have performed 5 different experiments as in Fig. 5A at different *DOPC* concentrations c_{DOPC} (Fig. 5B). The c_S values are a linear function of c_{DOPC}:

$$c_S = \frac{n_{L,S}}{n_{DOPC}} \cdot \left(\frac{1}{N_A V_{DOPC}} \cdot \frac{1}{K_P} + c_{DOPC} \right)$$

where the constant $n_{L,S}:n_{DOPC}$ is the molar ratio of *C12NO* located in the lipid phase and *DOPC* at the concentration c_S, N_A is the Avogadro constant, V_{DOPC} the molecular volume of *DOPC* in vesicles and K_P the partition koefficient of *C12NO* between the lipid bilayer phase and aqueous phase. The fit of c_S vs. c_{DOPC} data in Fig. 5B gave $n_{L,S}:n_{DOPC}$=0.76±0.08 and K_P=683±130. Using this K_P, the experimental data for *C12NO* in Fig. 3 and the data

as in Fig. 5A can be recalculated as a function of the *C12NO*:*DOPC* molar ratio **in bilayer** n_L:n_{DOPC} (Fig. 5C). Comparing the normalized turbidity $A_T/A_{T,0}$ ($A_{T,0}$ is the turbidity of *DOPC* ULVs without *C12NO*) and SANS shape parameter *r*, it is seen that bilayers in ULVs and/or in bilayer sheets (*r*=1) are present at the onset of solubilization $n_{L,S}$:n_{DOPC} and during the first half of stage II; the turbidity is not sensitive enough to register the transition to mixed cylindrical micelles (*r*=2). Theoretically, the transitions from bilayers to cylindrical micelles in lipid-surfactant aggregates occurs at the packing parameter $\delta=X_L V_{HL}/A_L L_{HL}+X_S V_{HS}/A_S L_{HS}=0.5$ [20, 21], where X_S is the molar fraction of surfactant and X_L=1-X_S of lipid, V_{Hi} is the hydrophobic volume, L_{Hi} the effective length of the hydrocarbon chain and A_i the surface area at the interface with the aqueous phase, and the indices *i*=*S* denote the surfactant (*C12NO)* and *i*=*L* the lipid (*DOPC*). We have calculated the volumes, lengths and areas from the SANS [22, 23] and volumetric [24] data and obtained that the theoretically predicted bilayer – cylindrical micelle transition should occur at the *C12NO*:*DOPC* molar ratio **in bilayer** n_L:$n_{DOPC}\approx$2: at about half of the rather broad transition from bilayers (*r*=1) to mixed cylindrical micelles (*r*=2) observed in SANS experiments (Fig. 5C). Summarizing – the solubilization proceeds in the following sequence of steps: bilayers in vesicles – (hypothetical holey bilayers in vesicles) – bilayer sheets (mixed discoid micelles?) – mixed cylindrical micelles – mixed globular micelles. This mechanism is most probably behind biocidal properties of *CnNO*s. Since the extent of *CnNO*-induced defect in bilayer per *CnNO* molecule decreases with the chain length *n* (Figs. 2 and 3) and the partition coefficient increases with *n* exponentially (Fig. 1), the final result is a cut-off type of dependence observed in biocidal potencies as in Fig. 1.

Not only the solubilizing effects, but also more subtle changes of bilayer physical properties at lower (subsolubilizing) *CnNO* concentrations can have important consequences on the bilayer biological functions. We have observed that *C12NO* increases the phosphohydrolase activity of the Ca^{2+}-transporting sarcoplasmic reticulum ATPase (SERCA) reconstituted into bilayers unilamellar DOPC vesicles at lower concentrations and decreases it at higher concentratio [23]. When reconstituted into bilayers from synthetic phospholipids, the activity of this transmembrane protein depends on the bilayer phase state, phospholipid hydrocarbon chain length, structure and charges of polar head groups of annular phospholipids surrounding the protein: a) the activity is practically zero in the solid-like (gel phase) bilayer, high in the fluid (liquid crystalline) bilayer, but the particular value of fluidity in the fluid state has no effect; b) for high activity, a fluid bilayer from lipids with zwitterionic head groups is required - charged lipids support low activities; c) lower activity is observed in lipids under conditions when they form non-bilayer aggregates in isolation; d) the activity in (zwitterionic) diacylphosphatidylcholines is highest in the fluid bilayer of DOPC, but lower in fluid bilayers with shorter or longer acyl chains [26, 27]. These results indicate, that the ATPase activity is modulated by a delicate interplay of several physical factors - bilayer thickness, hydrogen bonding potential and hydration, surface charge, dipole potential and curvature frustration of the bilayer seem to be the most important. When the activity is compared with bilayer physical parameters at the same bilayer *C12NO* concentration, the *C12NO*-induced increase in activity was observed in the range of *C12NO:DOPC* molar ratios in bilayers, where the bilayer thickness estimated by SANS decreases. In this range, the ^{31}P-NMR chemical shift anisotropy measured in MLV increases indicating an effect of *C12NO* on the *DOPC* N^+-P^- dipole orientation accompanied by a variation of the local bilayer dipole potential. The decrease in the ATPase activity is observed in the range of *C12NO:DOPC* molar ratios, where mixed tubular micelles were detected by SANS. It can be concluded that the effect of bilayer thickness decrease, which otherwise would result in the activity decrease, is compensated by the changes in the bilayer dipole potential; the

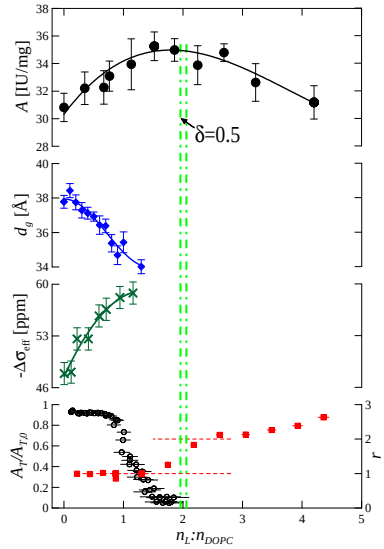

Fig. 6. Dependences of normalized turbidity $A_T/A_{T,0}$ (○), SANS shape parameter r (■), ^{31}P-NMR chemical shift anisotropy $-\Delta\sigma_{eff}$ (✖), bilayer thickness parameter d_g (◆), and Ca^{2+}-ATPase specific activity A (●) on the *C12NO*:*DOPC* molar ratio in bilayer, n_L:n_{DOPC}. The *C12NO*:*DOPC* molar ratio in bilayer at the bilayer – mixed tubular micelle transition (predicted by packing parameter δ) is delimited by dash-dotted vertical lines.

curvature frustration of the bilayer resulting in mixed tubular micelles in isolation, causes the decrease of the Ca^{2+}-ATPase activity.

The experiments above were performed with laterally homogeneous bilayers in the fluid state. The bilayer of biological membrane contains not only fluid regions, but also lateral domains which are solid-like – e.g. well known detergent-insoluble rafts. It is therefore interesting to study the *CnNO* interaction with solid-like bilayers. As a first step in this direction we have studied the influence of *CnNO* surfactants on the pretransition ($L_{\beta'}\rightarrow P_{\beta'}$) and the main gel-liquid crystal phase transition ($P_{\beta'}\rightarrow L_\alpha$) of dipalmitoylphosphatidylcholine (*DPPC*) bilayers in MLV using differential scanning calorimetry (DSC). $L_{\beta'}$ and $P_{\beta'}$ phases are solid-like, the L_α phase is fluid. Our results are summarized in Fig. 7. The temperature t_{m0} of the main phase transition, the temperature t_{p0} of the pretransition, and the calorimetric enthalpy ΔH_0 of the main phase transition determined from the thermogram of *DPPC* without *CnNO* were t_{p0}=35.48±0.20 °C, t_{m0}=41.53±0.02 °C and ΔH_0=34.8±1.6 kJ/mol, in agreement with data published previously in the literature. In the range of molar ratios *C12NO*:DPPC≤0.4 studied, both the main phase transition and pretransition of DPPC were gradualy shifted to lower temperatures and asymmetrically broadened (Figs. 7 A and B). Critical temperatures of the main- and pre- transition estimated from the maxima of thermal capacity c_p vs. t curves depend linearly on the *C12NO:DPPC* molar ratio in the studied range of concentrations (Fig. 7). The molar ratio *CnNO:DPPC*=0.2 was chosen to investigate the influence of the homologous series of *CnNO* (n=6-18) on the phase transitions of *DPPC*. As can be seen from Fig. 7, the efficiency of CnNO to decrease the phase transition temperatures of *DPPC* increases with n for n≤10 and reaches maxima for n=12-14. Longer homologs (n=16, 18) have an opposite effect causing an increase in phase

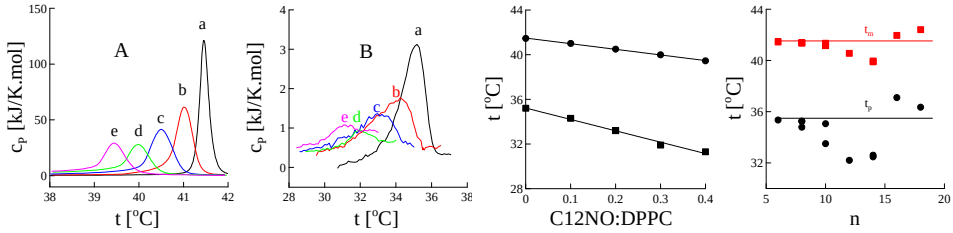

Fig. 7. Main phase transition (A) and pretransition (B) in *DPPC* bilayers (a) and in mixtures with molar ratios of *C12NO:DPPC*: 0.1 (b), 0.2 (c), 0.3 (d) and 0.4 (e), and dependences of DPPC phase transition temperatures as a function of *C12NO*:*DPPC* molar ratio (● — t_m, ■ — t_p) and as a function of *CnNO* alkyl length n (■ — t_m, ● — t_p) at *CnNO:DPPC*=0.2 molar ratio. The DPPC concentration was $6.81 \cdot 10^{-4}$ mol/l

transitions temperatures. Extending the van't Hoff theory of freezing point depression, it can be shown that this effect is connected with the surfactant partitioning into lipid bilayers [29] – the decrease of t_m occurs when the partition coefficient of surfactant between the fluid-state L_α bilayer and water, K_L, is higher than the partition coefficient of surfactant between the gel-state $P_{\beta'}$ bilayer and water, K_G, while the increase of t_m occurs when $K_L/K_G<1$. Similarly, when the partition coefficient K_G is higher than the partition coefficient of surfactant between the gel-state $L_{\beta'}$ bilayer and water, K_S, the decrease of t_p is observed and *vice versa*. The ability of long-chain CnNO surfactants to preferentially partition in the solid-like bilayers makes them very promising for further studies of raft properties.

As a conclusion we should like to stress that not only the partition equilibria and changes in bilayer physical properties of surfactants are important for their biological effects. Surfactants act on biological objects in time, so that their diffusion to their site of action and their metabolism during this diffusion are immensely important, especially when they have to pass series of hydrophilic and hydrophobic compartments. In the last case, the available concentration at the site of action can well display a cut-off type of dependence on the linear hydrophobic substituent [30]. The resulting biological effect is, consequently, a convolution of several mechanisms, and the structural perturbation of lipid bilayers, thogh very important, is just one of them.

Acknowledgements. We express our gratitude to Prof. dr. hab. inż. Kazimiera A. Wilk and to Prof. dr. hab. inż. Stanisław Witek for invitation to present our results at SURUZ 2007 Conference. This study was supported by the APVV-51-027404 grant and JINR project 07-4-1031-99/2008, and by the VEGA 1/3029/06 and 1/2280/05 grants.

REFERENCES

[1] HERRMAN K.W.: *J. Phys. Chem.* 68 (1964) 1540-1546
[2] LE MAIRE M., CHAMPEIL P., MOLLER J.V.: *Biochim. Biophys. Acta* 1508 (2000) 86-111
[3] DEVÍNSKY F., KOPECKÁ-LEITMANOVÁ A., ŠERŠEŇ F., BALGAVÝ P.: *J. Pharm. Pharmacol.* 42 (1990) 790-794
[4] MURÍN A., DEVÍNSKY F., KOLEKOVÁ A., LACKO I.: *Biológia (Bratislava)* 45 (1990) 521-531

[5] BUKOVSKÝ M., MLYNARČÍK D., ONDRÁČKOVÁ V.: *Int. J. Immunopharmacol.* 18 (1996) 423-426
[6] ŠERŠEŇ F., BALGAVÝ P., DEVÍNSKY F.: *Gen. Physiol. Biophys.* 9 (1990) 625-633
[7] ŠERŠEŇ F., GABUNIA G., KREJČÍŘOVÁ E., KRÁĽOVÁ K.: *Photosynthetica* 26 (1992) 205-212
[8] KARLOVSKÁ J., HAMMEL M., LAGGNER P., LACKO I., DEVÍNSKY F., BALGAVÝ P.: *Pharmazie* 60 (2005) 135-137
[9] MEYER H.H.: *Arch. Exp. Pathol. Pharmakol.* 42 (1899) 109-118
[10] OVERTON E.: *Studien Über Narkose, Zugleich Ein Beitrag Zur Allgemeinen Pharmakologie, Verlag Von Gustav Fischer, Jena*, Verlag von Gustav Fischer, Jena, 1901
[11] BALGAVÝ P., DEVÍNSKY F.: *Adv. Colloid Interface Sci.* 66 (1996) 23-63
[12] FILÍPEK J., GELIENOVÁ K., KOVÁCS P., BALGAVÝ P.: *Gen. Physiol. Biophys.* 12 (1993) 55-68
[13] GALLOVÁ J., ANDRIAMAINTY F., UHRÍKOVÁ D., BALGAVÝ P.: *Biochim. Biophys. Acta* 1325 (1997) 189-196
[14] UHRÍKOVÁ D., KUČERKA N., ISLAMOV A., GORDELIY V., BALGAVÝ P.: *Gen. Physiol. Biophys.* 20 (2001) 183-189
[15] KUČERKA N., NAGLE J.F., FELLER S.E., BALGAVÝ P.: *Phys. Rev. E* 69 (2004) 051903
[16] KUČERKA N., PENCER J., SACHS J.N., NAGLE J.F., KATSARAS J.: *Langmuir* 23 (2007) 1292-1299
[17] HRUBŠOVÁ A., KARLOVSKÁ J., DEVÍNSKY F., LACKO I., BALGAVÝ P.: *Čes. Slov. Farm.* 52 (2003) 299-305
[18] KARLOVSKÁ J., DEVÍNSKY F., LACKO I., GALLOVÁ J., BALGAVÝ P.: *Acta Facult. Pharm. Univ. Comenianae* 51 (2004) 119-128
[19] LICHTENBERG D., OPATOWSKI E., KOZLOV M.M.: *Biochim. Biophys. Acta* 1508 (2000) 1-19
[20] ISRAELACHVILI J., MITCHELL D.J., NINHAM B.W.: *J. Chem. Soc. , Faraday Trans. 2* 72 (1976) 1525-1568
[21] GOLTSOV A.N., BARSUKOV L.I.: *J. Biol. Phys.* 26 (2000) 27-41
[22] TIMMINS P.A., HAUK J., WACKER T., WELTE W.: *FEBS Lett.* 280 (1991) 115-120
[23] KARLOVSKÁ J., UHRÍKOVÁ D., KUČERKA N., TEIXEIRA J., DEVÍNSKY F., LACKO I., BALGAVÝ P.: *Biophys. Chem.* 119 (2006) 69-77
[24] UHRÍKOVÁ D., RYBÁR P., HIANIK T., BALGAVÝ P.: *Chem. Phys. Lipids* 145 (2007) 97-105
[25] KARLOVSKÁ J., LOHNER K., DEGOVICS G., LACKO I., DEVÍNSKY F., BALGAVÝ P.: *Chem. Phys. Lipids* 129 (2004) 31-41
[27] LEE A.G., EAST J.M., BALGAVÝ P.: *Pesticide Sci.* 32 (1991) 317-327
[28] LEE A.G.: *Biochim. Biophys. Acta* 1666 (2004) 62-87
[29] GALLOVÁ J., BÁGEĽOVÁ J., ČIŽMÁRIK J., BALGAVÝ P. *Collect. Czech. Chem. Commun.* 60 (1995) 763-780
[30] BALÁŽ Š., ŠTURDÍK E., ROSENBERG M., AUGUSTÍN J., ŠKÁRKA B. *J. Theor. Biol.* 131 (1988) 115-134